APPLICATION OF THE PEROVSKITE CERAMICS TO CONDITIONING OF THE LONG-LIVED FRACTION OF HLW

N.E. Cherniavskaya[1], S.V. Chizhevskaya, A.V. Ochkin
University of Chemical Engineering of Russia,
Miusskaya 9, Moscow 125047 RUSSIA

S.V. Stefanovsky
SIA "Radon", 7th Rostovskii per. 2/14, Moscow 119121 RUSSIA, itbstef@cityline.ru

ABSTRACT

High level waste (HLW) partitioning concept includes separation of a long-lived fraction following by its immobilization in ceramics. Improved process flow sheet suggested for implementation at PA "Mayak" implies production of a long-lived HLW fraction with rare earth elements (REE) as major components, Am and Cm as minor constituents, and only traces of U, Pu, and corrosion products (iron group elements). Because most of the elements occurred are trivalent, one of the most promising host phase is supposed to be REE aluminate or ferrate with perovskite structure. Major advantages of the perovskite are incorporation of trivalent REEs and actinides, simultaneous incorporation of residual corrosion products, flexibility of perovskite structure allowing accommodation of traces of tetravalent actinides (U, Pu), high chemical durability, and high HLW volume reduction. High melting points of the perovskites makes problematic melting route, therefore, cold pressing and sintering method is more preferable. In order to reduce sintering temperature pre-treatment of ceramic batches with high mechanical energy has been studied.

Ceramic samples with formulations $Ca_{1-x}Gd_xTi_{1-x}Al_xO_3$ produced from mechanically activated batches were examined with X-ray diffraction (XRD) and scanning electron microscopy with energy dispersive system (SEM/EDS). Oxide mixtures were mechanically activated, compacted in pellets and sintered at 1350 ^{0}C. Application of the mechanical activation reduced sintering temperature by 100-200 ^{0}C (from 1450-1550 to 1300-1400 ^{0}C) yielding product with high quality. Some samples were doped with ^{90}Sr and ^{241}Am. Leach rates of these radionuclides measured by PCT test were found to be ranged between ~10^{-4} and 10^{-6} g/(m^2*day).

INTRODUCTION

Currently the HLW partitioning concept is considered to be implemented in various countries including Russia [1-3]. As a result of the HLW partitioning volume of waste containing the longest lived radionuclides and requiring to be stored for hundreds of thousands years is reduced by factors of about 20. Major elements, whose radionuclides are present in the long-lived fraction, are rare earths (REE) mainly lanthanides (La...Gd) and actinides (U...Cm). To immobilize this fraction various matrices based on zirconolite [4-6], zircon [7], cubic zirconia [8], murataite [9] as well as perovskite [10,11] were proposed. These phases are long-term stable under geologic conditions including stability under α-decay of natural uranium and thorium isotopes. An advantage of perovskite is capability to trivalent lanthanides and actinides

[1] Current address: SIA Radon, 7th Rostovskii per. 2/14, Moscow 119121 RUSSIA

substitution for calcium in its structure. Lanthanides are normally trivalent except cerium and terbium which can be tetravalent and europium which can be divalent. Americium and curium are normally also trivalent, and plutonium may be trivalent as well under reducing conditions.

Perovskites are mineral group with general formula ABO_3 with cubic or orthorhombic symmetry for compounds with $A^{2+}B^{4+}O_3$ formulation and rhombohedral or orthorhombic symmetry for compounds with $A^{3+}B^{3+}O_3$ formulation [12]. Compositions of the natural perovskites are comprised by quaternary system with perovskite ($CaTiO_3$), loparite ($Na_{0.5}REE_{0.5}TiO_3$), lueshite ($NaNbO_3$), and tausonite ($SrTiO_3$) as end members (minals) [13]. It is considered that Sr^{2+}, REEs, U^{4+}, and Na^+ enter $CaTiO_3$ based solid solution as $SrTiO_3$, $REE^{3+}AlO_3$ or $REE^{3+}Ti^{3+}O_3$, $Ca_{0.5}U^{4+}{}_{0.5}Ti^{3+}O_3$, and $Na^+{}_{0.5}REE^{3+}{}_{0.5}Ti^{4+}O_3$, respectively [12]. Major isomorphic exchange schemes in the natural and synthetic perovskites are $Ca^{2+} \leftrightarrow Sr^{2+}$, $2Ca^{2+} \leftrightarrow Na^+ + REE^{3+}$, $Ca^{2+} + Ti^{4+} \leftrightarrow REE^{3+} + (Al,Fe,Ti)^{3+} \leftrightarrow Na^+ + (Nb,Ta)^{5+}$ as well as vacancy mechanisms.

Perovskites belonging to the same symmetry group form continuous solid solutions, for example orthorhombic $CaTiO_3$ with other orthorhombic phases ($REEAlO_3$), but in the other cases miscibility break may occur.

Isomorphism in the Gd-containing $CaTiO_3$ was investigated in ref. [14]. It has been shown that isomorphic capacity of perovskite with respect to gadolinium is negligible in the absence of Al^{3+} ions being charge compensator by scheme: $Ca^{2+} + Ti^{4+} = Gd^{3+} + Al^{3+}$: *x* value doesn't exceed 0.15-0.25 formula units depended on the substitution mechanism chosen. At the same time perovskite compositions in the series $Ca_{1-x}Gd_xTi_{1-x}Al_xO_3$ form continuous solid solution and perovskite grains composition always corresponded to specified *x* value. Samples preparation conditions (sintering at 1300 ^{0}C for 2 hours, re-milling, compaction, and sintering at 1550 ^{0}C for 1 week) in ref. [14] reached in practice an equilibrium state. Samples synthesis conditions in actual HLW solidification process differs essentially from equilibrium. In the present work we studied some regularities of phase formation in perovskite-based ceramics under conditions close to actual cold pressing and sintering technological process and the effect of mechanical activation on phase composition and elements partitioning among co-existing phases in the ceramics produced.

EXPERIMENTAL

The ceramic samples with $Ca_{1-x}Gd_xTi_{1-x}Al_xO_3$ formulations were prepared by three routes (Table I):

- Milling of Ca, Gd, Ti, and Al oxides in an agate mortar, compaction in pellets under pressure of 250 Mpa, heat-treatment to 1350 ^{0}C for 3 hours, exposure at 1350 ^{0}C for 2 hours, cooling down to room temperature in air (the samples marked "a" in Table I));
- Milling of Ca, Gd, Ti, and Al oxides in an agate mortar, mechanical treatment in an apparatus with rotating magnetic field (ARMF) for 10 min., followed by treatment as indicated above (the samples marked "b" in Table I);
- Milling of Ca, Gd, Ti, and Al oxides in an agate mortar, mechanical treatment in the ARMF for 15 min, followed by treatment as indicated above (the samples marked "c" in Table I).

Table I. The samples in series $Ca_{1-x}Gd_xTi_{1-x}Al_xO_3$ studied.

Sample	*x*, formula units	Batch preparation
1b	0	Batch treatment in the ARMF for 10 min.
2b	0.05	Batch treatment in the ARMF for 10 min.
3a	0.1	Batch milling in mortar
3b	0.1	Batch treatment in the ARMF for 10 min.
4b	0.2	Batch treatment in the ARMF for 10 min.
4c	0.2	Batch treatment in the ARMF for 15 min.
5a	0.3	Batch milling in mortar
5b	0.3	Batch treatment in the ARMF for 10 min.
5c	0.3	Batch treatment in the ARMF for 15 min.
6b	0.4	Batch treatment in the ARMF for 10 min.
6c	0.4	Batch treatment in the ARMF for 15 min.
7b	0.5	Batch treatment in the ARMF for 10 min.
8c	0.6	Batch treatment in the ARMF for 15 min.
9c	0.7	Batch treatment in the ARMF for 15 min.
10c	0.8	Batch treatment in the ARMF for 15 min.
11c	0.9	Batch treatment in the ARMF for 15 min.
12c	1.0	Batch treatment in the ARMF for 15 min.

Some samples were doped with ^{90}Sr and ^{241}Am to measure leach rates of these radionuclides. The samples produced were examined with X-ray diffraction (XRD, diffractometer DRON-4, Cu K_α radiation) and scanning electron microscopy with energy dispersive system (SEM/EDS) using an analytical system JSM-5300+Link ISIS. Leach rates of ^{90}Sr and ^{241}Am were measured using a PCT test [15].

RESULTS AND DISCUSSION

As follows from XRD data (Figures 1-3) perovskite with rhombic lattice symmetry (space group *Pnma*) is predominant phase in all the samples. In the samples produced by sintering at 1350 ^0C major phase was found to be normal perovskite with chemical composition close to $CaTiO_3$ (major reflections are d = 2.69-2.70, 1.91, and 1.55 Å). Moreover, in the samples with high Gd and Al content an extra perovskite structure phase (*Pnma*) with composition close to $GdAlO_3$ was observed. Its major reflections are d = 3.71-3.73, 2.63-2.64, 1.86-1.87 Å. This phase was revealed in the samples ## 3b?, 4b, 5b, 6b, and 7b. In the latter sample peaks intensity of the given phase exceeds reflections of normal perovskite ($CaTiO_3$). Occurrence of two isostructural phases with different compositions may point to either limited miscibility in the system $CaTiO_3$-$GdAlO_3$ or incomplete mineral formation in the ceramic batches owing to what perovskite phases with strongly different compositions are co-existing in the samples produced. As follows from XRD patterns, the $GdAlO_3$ phase occurred in the samples at $x \geq 0.2$. Moreover, rutile TiO_2 (major reflections are d = 3.24-3.25, 2.48-2.49, and 1.68-1.69 Å), pyrochlore-structured gadolinium titanate (major reflections are d = 2.92-2.94 and 1.79-1.80 Å), and calcium oxide (d = 2.75-2.77, 2.40, and 1.69-1.70 Å) were present. Rutile was reliably identified in the samples ## 3a, 4b, 5a, 6b, and 7b. Lime was found in the samples from non-activated batches only (##3a and 5a).

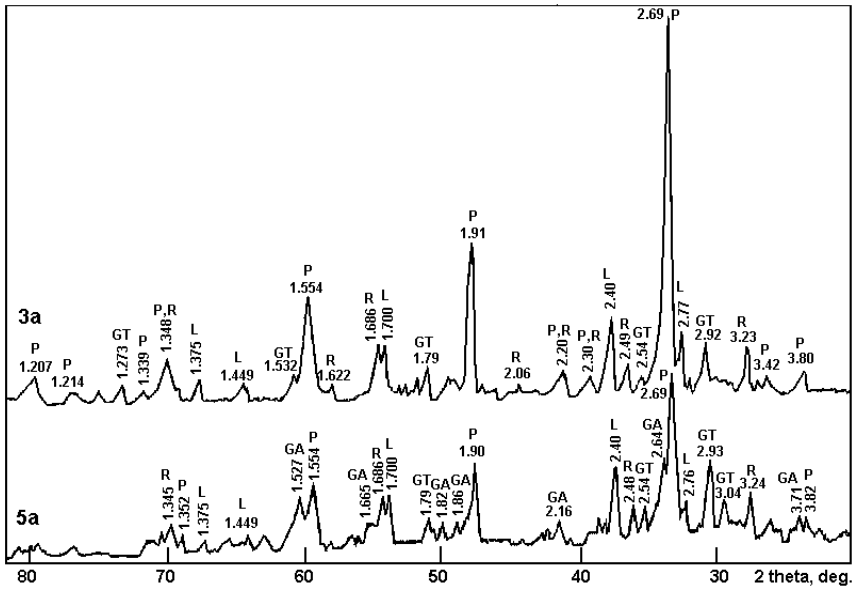

Fig. 1. XRD patterns of the ceramic samples prepared from batches milled in mortar. Compositions are given in Table I. GA – perovskite structure gadolinium titanate, GT – pyrochlore structure gadolinium titanate, L – lime, P – perovskite, R – rutile.

A set and relative extra phases content vary from sample to sample. The following regularities are clearly established. Amount of the $GdAlO_3$ phase grows with increase of Gd and Al concentrations in the system. This reaches maximum value in the sample #7b (x=0.5), where the given phase content probably exceeds normal perovskite ($CaTiO_3$) content. This conclusion, however, requires verification, because phases relation evaluation on the basis of their peaks intensities is only rough.

Lime reflections are mostly expressed on XRD patterns of the samples ## 3a and 5a produced from powders milled in mortar. No this phase was found in the samples ## 3b and 5b with the same compositions but produced from mechanically activated powders. Occurrence of rutile in the samples ## 3a and 5a points to incomplete perovskite formation by reaction $CaO + TiO_2 = CaTiO_3$. Thus, mechanical activation of initial batch is believed to be really facilitates perovskite synthesis if the rest of parameters (particles size, intermixing quality, duration and synthesis temperature) are the same.

Regularities of the pyrochlore structure phase ($Gd_2Ti_2O_7$) formation in the samples are less clear. Marked amount of the given phase was observed in the samples ## 3a and 5a, that can be explained by incomplete reactions like in the case of rutile and lime. Moreover, minor content of this phase was observed in the samples ## 5b (?), 6b, and 7b with the highest Gd content.

Rutile was found in the samples ## 3a and 5a, where this was unreacted source component. Moreover, rutile reflexes are observed on XRD pattern of normal perovskite (the sample #1b).

SEM/EDS study was carried out for the sample #3b containing two perovskite and pyrochlore-structured phases. SEM images (Figure 4) demonstrate several types of crystalline grains differed in chemical composition (Table II). This sample has significant porosity.

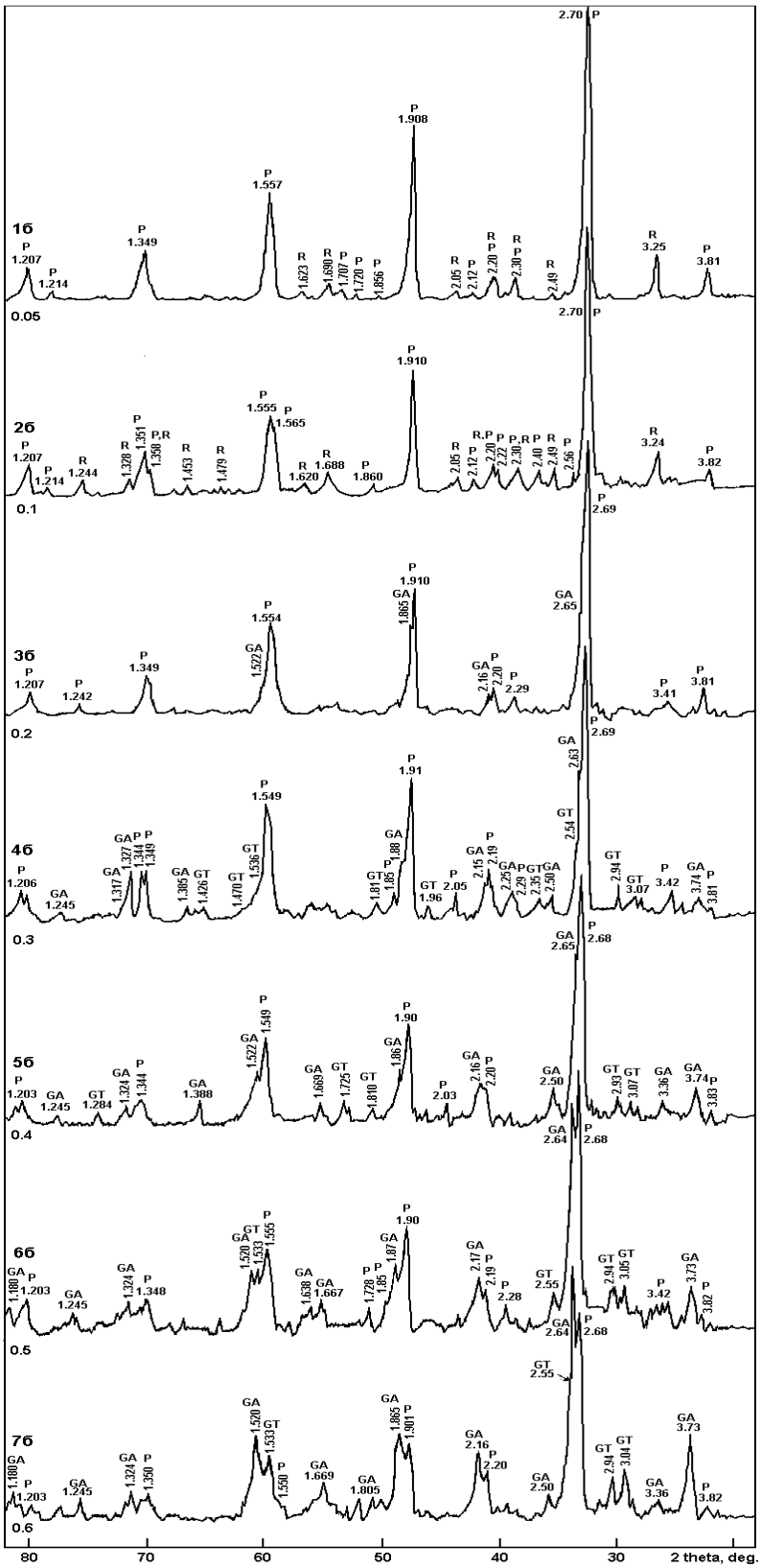

Fig. 2. XRD patterns of the ceramic samples prepared from batches activated in the ARMF for 10 min. Compositions are given in Table I. Phase symbols are as on Figure 1.

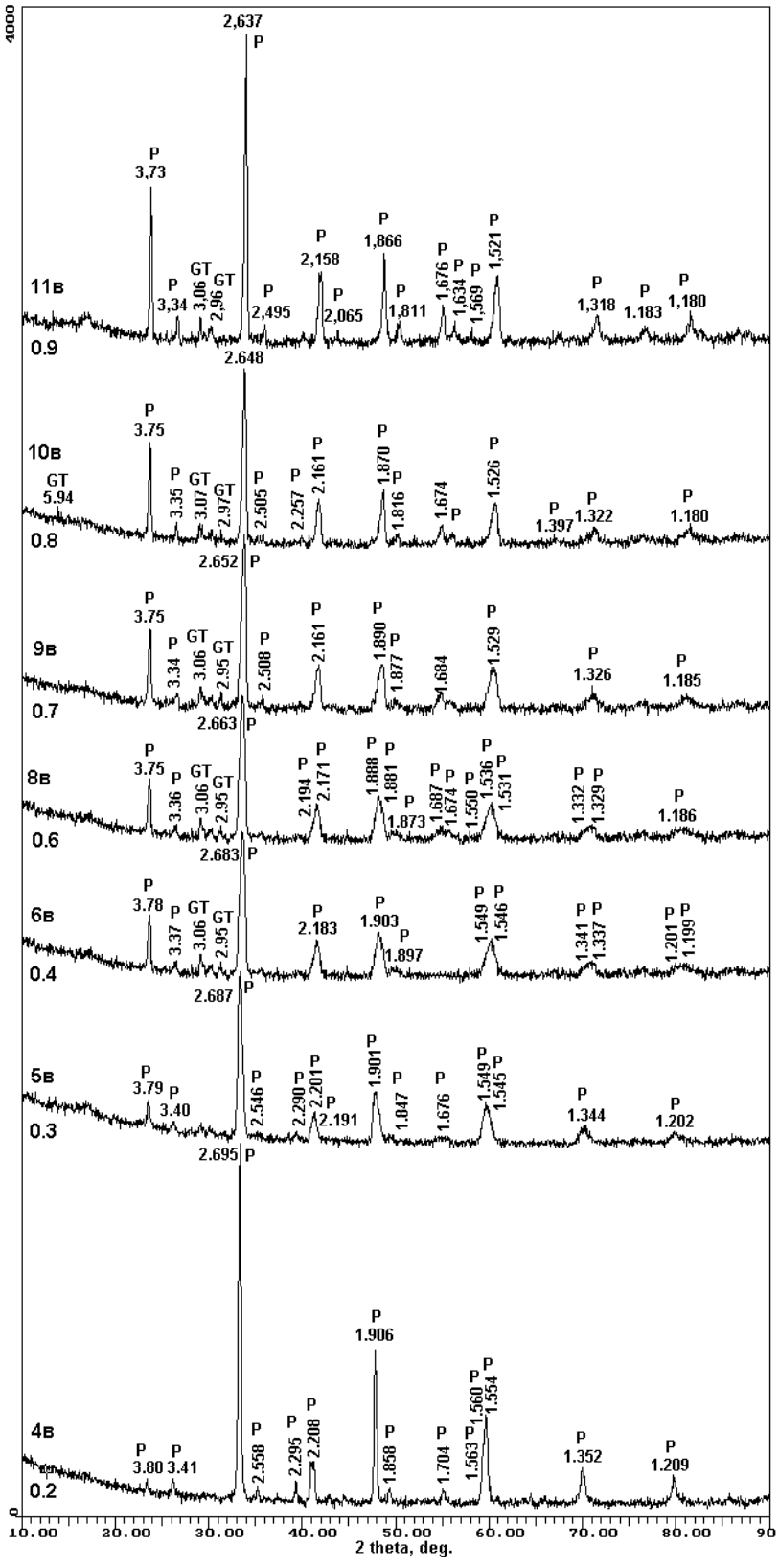

Fig. 3. XRD patterns of the ceramic samples prepared from batches activated in the ARMF for 15 min. Compositions are given in Table I. Phase symbols are as on Figures 1 and 2.

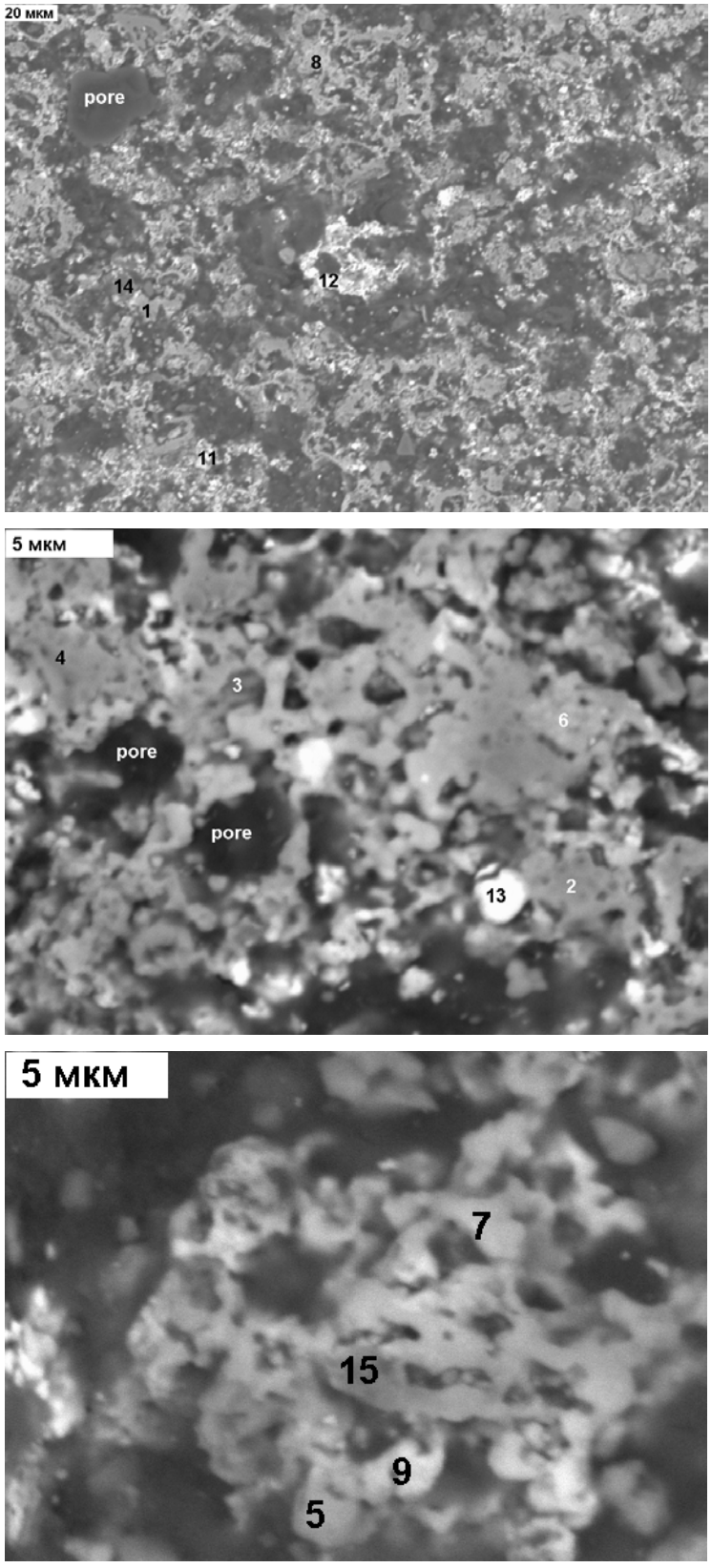

Fig. 4. SEM-images of the sample #3b at various magnifications.
Numbers on pictures correspond to EDS probes in Table II; mkm = μm.

Table II. Chemical compositions and formulae of the phases in the sample # 3b.

Oxides	1	2	3	4	5	6	7	8	9	10	11	12	13	14	15
	Oxides content, wt.%														
Al_2O_3	0.7	1.3	2.2	3.7	4.8	6.4	6.7	7.5	13.1	22.5	11.0	0.6	0.5	75.5	47.7
CaO	37.4	38.3	23.2	32.9	25.2	26.9	19.5	10.1	11.0	12.4	18.1	3.0	1.6	20.2	14.4
TiO_2	52.9	55.3	40.0	45.3	36.5	40.0	34.5	13.2	15.2	13.3	3.9	1.8	29.5	0.6	20.2
Gd_2O_3	5.6	6.5	27.0	14.0	17.4	23.1	30.5	50.6	49.6	48.5	58.9	93.6	64.2	1.5	16.8
Sum	96.6	101.4	92.4	95.9	83.9	96.4	91.2	81.4	88.9	96.7	91.9	99.0	95.8	97.8	99.1
Ions	Formula units														
Al^{3+}	0.03	0.04	0.08	0.10	0.18	0.20	0.23	0.38	0.58	0.81	0.53	0.04	0.04	3.97	2.84
Ca^{2+}	0.97	0.96	0.72	0.90	0.82	0.80	0.62	0.46	0.42	0.40	0.78	0.18	0.16	0.94	0.79
Ti^{4+}	0.97	0.96	0.88	0.90	0.82	0.80	0.80	0.42	0.42	0.30	0.11	0.08	1.95	0.00	0.75
Gd^{3+}	0.03	0.04	0.25	0.10	0.18	0.20	0.31	0.72	0.58	0.49	0.80	1.76	1.87	0.00	0.28
Sum	2.00	2.00	1.93	2.04	2.00	2.00	1.96	1.98	2.00	2.00	2.22	2.06	4.02	4.91	4.66
O^{2-}	3.00	3.00	3.00	3.00	3.00	3.00	3.00	3.00	3.00	3.00	3.00	3.00	7.00	7.00	7.00
Phases	P	P	P+G?	P	P	P	P+GT	P+G	P	P+A	P?+G?	G	GT	CA	CAT

A – alumina (corundum) Al_2O_3, CA – calcium aluminate $CaAl_4O_7$, CAT – calcium aluminotitanate (CAT phase) $Ca(Ti,Al)_4O_7$, G – gadolinium oxide Gd_2O_3, GT – pyrochlore structure gadolinium titanate $Gd_2Ti_2O_7$, P – perovskite solid solution ($CaTiO_3$-$GdAlO_3$).

Major bulk of the sample is composed of perovskite crystals (gray colored on SEM images) with variable chemical composition (Table II, *1-10*) corresponding to continuous solid solution $Ca_{1-x}Gd_xTi_{1-x}Al_xO_3$ within the range $0 \le x \le 0.6$ (within experimental error). Grains ## 3 and 10 are aggregates of perovskite and Gd and Al oxides, respectively. Grain # 11 is probably aggregate of strongly defect perovskite and Gd oxide. Some grains (white colored on SEM images) are gadolinium oxide (Table II, *12*) and pyrochlore structure gadolinium titanate (Table II, *13*). Individual grains of calcium aluminate and aluminotitanate (CAT phase) also occurred.

In the whole, it should be noted that, in spite of incomplete mineral formation reactions, the sample # 3b is mainly composed of perovskite solid solution as well as pyrochlore structure phase, i.e. phases whose long-term stability is reliably proven [12,13]. Minor CAT phase doesn't contain gadolinium.

Major reflexes on XRD patterns of seven ceramic samples with $Ca_{1-x}Gd_xTi_{1-x}Al_xO_3$ formulation at x = 0.2 (#4c), 0.3 (#5c), 0.4 (#6c), 0.6 (#8c), 0.7 (#9c), 0.8 (#10c), and 0.9 (#11c) produced by sintering of pellets from powders treated in the ARMF for 15 min. at the same temperature (1350 ^{0}C) are due to perovskite structure phase (*Pnma*). At $x \le 0.4$ peaks locations and intensities are close to typical of normal perovskite ($CaTiO_3$ – JCPDS 22-153), at $x \ge 0.6$ peaks positions and intensities corresponds approximately to gadolinium aluminate ($GdAlO_3$ – JCPDS 30-15) also with perovskite structure. As seen from Figure 3, increase of the x value from 0.2 to 0.9 shifts the strongest peak position from 2.687 to 2.637 Å, i.e. from the value close to tabulated for $CaTiO_3$ (2.701 Å) to the value being characteristic of $GdAlO_3$ (2.633 Å). Such a permanent XRD pattern variation points to formation of continuous solid solutions in the system $CaTiO_3$-$GdAlO_3$. This is in a good agreement with reference data [14].

As follows from experimental data, mechanical treatment of oxide batch in the ARMF increases target phase yield at the following sintering as compared to untreated batch at the same sintering temperature (currently 1350 ^{0}C). So, comparison of XRD patterns of the samples ## 3a and 3b, and 5a and 5b shows that ceramic samples prepared from batches activated in the ARMF for 10 min. are free of unreacted phases.

Because the samples from batches milled in mortar had low mechanical integrity [16], leach rates of radionuclides were measured from the samples prepared from mechanically activated batches only. Results were treated using an eq. (1):

$$W = a_1 exp(-b_1 t) + a_2, \qquad \text{(Eq. 1)}$$

where W is leach rate (g/(m^2·day), a_1, b_1, and a_2 are coefficient determined from experimental data, and t is leaching test duration (days).

The first member in the equation describes leaching from metastable phases in the initial period of leaching. The second member (a_2) is equilibrium leach rate. Results are given in Tables III and IV.

The ^{90}Sr equilibrium leach rate from the ceramic samples in the series:$Ca_{1-x}Gd_xTi_{1-x}Al_xO_3$ elevates insignificantly as Gd content increases within the range $0 < x \le 0.3$ and then remains approximately constant. The ^{241}Am leach rate reduces strongly (by factor of about 30) at low Gd additive (x=0.05) as compared to perovskite with nominal composition ($CaTiO_3$), then it remains approximately constant within the range $0.05 < x \le 0.3$, grows by a factor of about 3 within the range $0.3 < x \le 0.6$, and reduces at high Gd content ($0.6 < x \le 1$). The reasons of these effects should be looked for features of microcomponents incorporation in the structure of the ceramics. Leach rate of ^{90}Sr from the pyrochlore structure phase ($Gd_2Ti_2O_7$) are at the same level as from

Table III. ^{90}Sr leach rates from the ceramic samples in the series $Ca_{1-x}Gd_xTi_{1-x}Al_xO_3$ and $Gd_2Ti_2O_7$.

Leaching duration, days	Leach rate, W, g/(m^2·day)					
	2b (x=0,05)	4c (x=0,2)	6c (x=0,4)	7c (x=0,5)	12c (x=1) $GdAlO_3$	$Gd_2Ti_2O_7$
1	$1{,}61\cdot10^{-3}$	$2{,}22\cdot10^{-2}$	$9{,}60\cdot10^{-2}$	$5{,}78\cdot10^{-2}$	$2{,}11\cdot10^{-3}$	-
2	$1{,}98\cdot10^{-3}$	$6{,}36\cdot10^{-3}$	$2{,}02\cdot10^{-2}$	$1{,}10\cdot10^{-2}$	$4{,}32\cdot10^{-4}$	$2{,}00\cdot10^{-3}$
3	$7{,}51\cdot10^{-4}$	$3{,}64\cdot10^{-3}$	$1{,}17\cdot10^{-4}$	$4{,}89\cdot10^{-3}$	$2{,}64\cdot10^{-4}$	$1{,}01\cdot10^{-3}$
4	$5{,}40\cdot10^{-4}$	$9{,}91\cdot10^{-4}$	$2{,}57\cdot10^{-3}$	$2{,}39\cdot10^{-3}$	$1{,}21\cdot10^{-4}$	$6{,}58\cdot10^{-4}$
5	$6{,}71\cdot10^{-4}$	$8{,}40\cdot10^{-4}$	$1{,}89\cdot10^{-3}$	$2{,}01\cdot10^{-3}$	$9{,}86\cdot10^{-5}$	$5{,}21\cdot10^{-4}$
6	$5{,}72\cdot10^{-4}$	$3{,}03\cdot10^{-4}$	$1{,}17\cdot10^{-3}$	$9{,}74\cdot10^{-4}$	$1{,}40\cdot10^{-4}$	$6{,}81\cdot10^{-4}$
7	-	$4{,}61\cdot10^{-4}$	$4{,}27\cdot10^{-4}$	$7{,}75\cdot10^{-4}$	$2{,}64\cdot10^{-5}$	$5{,}69\cdot10^{-4}$
8	$1{,}34\cdot10^{-4}$	$3{,}55\cdot10^{-4}$	$2{,}32\cdot10^{-4}$	$4{,}39\cdot10^{-4}$	$2{,}76\cdot10^{-5}$	$5{,}78\cdot10^{-4}$
9	$9{,}70\cdot10^{-5}$	$2{,}23\cdot10^{-4}$	$2{,}26\cdot10^{-4}$	$3{,}67\cdot10^{-4}$	$3{,}65\cdot10^{-5}$	-
10	$7{,}31\cdot10^{-5}$	$1{,}76\cdot10^{-4}$	-	$2{,}93\cdot10^{-4}$	-	-
$a_1\cdot10^3$	0,08±0,01	63,1±3,4	325±22	236±17	5,1±0,08	-
b_1	0,50	1,08	1,27	0,45	1,11	-
$a_2\cdot10^4$	0,65±0,22	2,66±0,63	3,3±1,8	5,6±1,7	3,6±1,0	5,90±0,74

Table IV. ^{241}Am leach rates from the ceramic samples in the series $Ca_{1-x}Gd_xTi_{1-x}Al_xO_3$ and $Gd_2Ti_2O_7$.

Leaching duration, days	Leach rate W, g/(m^2·day)									
	1b (x=0) $CaTiO_3$	2b (x=0,05)	3b (x=0,1)	4c (x=0,2)	5c (x=0,3)	8c (x=0,6)	9c (x=0,7)	11c (x=0,9)	12c(x=1) $GdAlO_3$	$Gd_2Ti_2O_7$
1	$3{,}50\cdot10^{-3}$	$1{,}16\cdot10^{-5}$	$1{,}19\cdot10^{-5}$	$4{,}32\cdot10^{-5}$	$4{,}31\cdot10^{-6}$	$1{,}86\cdot10^{-5}$	$4{,}18\cdot10^{-5}$	$2{,}10\cdot10^{-5}$	$1{,}41\cdot10^{-4}$	-
2	$2{,}07\cdot10^{-3}$	$6{,}98\cdot10^{-6}$	$1{,}92\cdot10^{-5}$	$3{,}94\cdot10^{-5}$	$6{,}02\cdot10^{-6}$	$1{,}64\cdot10^{-5}$	$2{,}83\cdot10^{-5}$	-	$6{,}48\cdot10^{-5}$	$1{,}28\cdot10^{-3}$
3	$9{,}89\cdot10^{-5}$	$5{,}02\cdot10^{-6}$	-	$2{,}09\cdot10^{-5}$	$8{,}85\cdot10^{-6}$	$1{,}13\cdot10^{-5}$	$1{,}19\cdot10^{-5}$	$1{,}97\cdot10^{-5}$	$2{,}03\cdot10^{-5}$	$1{,}10\cdot10^{-3}$
4	$1{,}02\cdot10^{-4}$	$4{,}08\cdot10^{-6}$	$1{,}34\cdot10^{-5}$	-	$5{,}91\cdot10^{-6}$	$1{,}20\cdot10^{-5}$	-	$1{,}56\cdot10^{-5}$	$2{,}15\cdot10^{-5}$	$1{,}07\cdot10^{-3}$
5	$9{,}62\cdot10^{-5}$	$3{,}55\cdot10^{-6}$	$4{,}13\cdot10^{-6}$	$1{,}73\cdot10^{-5}$	-	$2{,}30\cdot10^{-5}$	$1{,}41\cdot10^{-5}$	-	$6{,}43\cdot10^{-6}$	$1{,}17\cdot10^{-3}$
6	$9{,}48\cdot10^{-5}$	$3{,}19\cdot10^{-6}$	$4{,}15\cdot10^{-6}$	$6{,}36\cdot10^{-6}$	$5{,}02\cdot10^{-6}$	$1{,}08\cdot10^{-5}$	$8{,}64\cdot10^{-6}$	$1{,}33\cdot10^{-5}$	$4{,}80\cdot10^{-6}$	$7{,}36\cdot10^{-4}$
7	$1{,}03\cdot10^{-4}$	$3{,}24\cdot10^{-6}$	$4{,}32\cdot10^{-6}$	-	$2{,}67\cdot10^{-6}$	$8{,}11\cdot10^{-6}$	$1{,}14\cdot10^{-5}$	$7{,}97\cdot10^{-6}$	$4{,}06\cdot10^{-6}$	-
8	$1{,}01\cdot10^{-4}$	-	$1{,}05\cdot10^{-5}$	$4{,}97\cdot10^{-6}$	$3{,}31\cdot10^{-6}$	$7{,}13\cdot10^{-6}$	$1{,}47\cdot10^{-5}$	$8{,}66\cdot10^{-6}$	$5{,}94\cdot10^{-6}$	$4{,}56\cdot10^{-4}$
9	-	-	$3{,}22\cdot10^{-6}$	$3{,}28\cdot10^{-6}$	$4{,}32\cdot10^{-6}$	$1{,}30\cdot10^{-6}$	$1{,}54\cdot10^{-5}$	$7{,}99\cdot10^{-6}$	-	$4{,}37\cdot10^{-4}$
10		-	$1{,}07\cdot10^{-5}$	$5{,}67\cdot10^{-6}$	$2{,}83\cdot10^{-6}$	-	$8{,}30\cdot10^{-6}$	$1{,}07\cdot10^{-5}$	$7{,}92\cdot10^{-6}$	$7{,}18\cdot10^{-4}$
11		-	$8{,}42\cdot10^{-6}$	$3{,}07\cdot10^{-6}$	-	-	-	-	$6{,}31\cdot10^{-6}$	$4{,}39\cdot10^{-4}$
$a_1\cdot10^5$	11760± 430	17,5±2,6	1,39± 0,57	7,10± 0,69	-	-	7,39± 0,88	2,02± 0,36	33,9±1,1	163±24
B_1	1,77	0,87	0,27	0,50		-	0,87	0,25	0,90	0,25
$a_2\cdot10^6$	96.2±4.3	3.05±0.05	5.1±1.9	5.4±1.7	4.6±1.9	13.4±4.9	11.5±1.4	7.2±1.3	5.9±1.3	386±72

ceramics with x=0.5. At the same time ^{241}Am leach rate from the pyrochlore phase is higher by factor of about 4 than from $CaTiO_3$, and by 30-70 times higher than from Gd-substituted perovskites. Therefore, occurrence of this phase in the perovskite ceramics seems to be undesirable.

CONCLUSIONS

All the samples studied are polyphase ceramics composed of major perovskite solid solution $CaTiO_3$-$GdAlO_3$ and minor extra phases: $Gd_2Ti_2O_7$, TiO_2, and CaO (in the samples from non-activated batches only). Therefore, composition of the perovskite ceramics produced can not be corresponding to specified stoichiometric formulae. Actual phases composition of the samples should be taken into account at analysis of leaching test results. In particular, occurrence of minor pyrochlore phase in the perovskite ceramics is undesirable because ^{241}Am leach rate from this phase is higher than from Gd-substituted perovskites by about 30-70 times.

REFERENCES

1. Y.V. Glagolenko, E.G. Dzekun, E.G. Drozhko, et. al., Quest. Rad. Safety ((Russ) [2] (1996) 3-10.
2. M. Horie, T. Tanaka, Y. Ikenaga, Waste Management '96 Proc. Rep. 35-5. CD Rom.
3. N.S. Babaev, A.N. Sinev, I.A. Sobolev, et. al., Waste Management '97 Proc. Rep. 07-04. CD Rom.
4. E.R. Vance, B.D. Begg, R.A. Day, C.J. Ball, Mat. Res. Soc. Symp. Proc. **353** (1995) 767-774.
5. S.V. Yudintsev, B.I. Omelianenko, S.V. Stefanovsky et. al., Adv. Mater (Russ) [1] (1998) 91-100.
6. S.V. Stefanovsky, S.V. Yudintsev, B.S. Nikonov, et. al., SPECTRUM '98, **2** (1998) 834-839.
7. B.E. Burakov, E.B. Anderson, V.S. Rovsha, et. al., Mat. Res. Soc. Symp. Proc. **412** (1996) 33-39.
8. B.E. Burakov, K.B. Helean, V.A. Korolev, et. al., Mat. Res. Soc. Symp. Proc. **506** (1998) 95-100.
9. N.P. Laverov, I.A. Sobolev, S.A. Dmitriev, et. al., High Level Radioactive Waste Management. Proc. Eighth Int. Conf. Las Vegas, Nevada, May 11-14, 1998. pp. 613-615.
10. B.D. Begg, E.R. Vance, G.R. Lumpkin, Mat. Res. Soc. Symp. Proc. **506** (1998) 79-86.
11. A.V. Ochkin, S.V. Chizhevskaya, S.V. Stefanovsky, et. al., SPECTRUM '98, **2** (1998) pp.796-801.
12. A.E. Ringwood, S.E. Kesson, K.D. Reeve, et. al., Radioactive Waste Forms for the Future, eds. W. Lutze and R.C. Ewing. Elsevier Science Publishers B.V., 1988. pp. 233-334.
13. G.R. Lumpkin, M. Colella, K.L. Smith, et. al., Mat. Res. Soc. Symp. Proc. **506** (1998) 207-214.
14. E.R. Vance, R.A. Day, Z. Zhang, et. al., J. Solid State Chem. **124** (1996) 77-82.
15. ASTM Standard C1285-94. ASTM, Philadelphia, PA (1994).
16. S.V. Chizhevskaya, N.E. Cherniavskaya, A.V. Ochkin, A.M. Chekmarev, S.V. Stefanovsky, Mat. Res. Soc. Symp. Proc. (2001), in press.